The morphology of nodal lines–random waves *vs* percolation

G Foltin†‡, S Gnutzmann§, U Smilansky†

†Department of Physics of Complex Systems, Weizmann Institute of Science, Rehovot 76100, Israel

§Institut für Theoretische Physik, Freie Universität Berlin, Arnimallee 12, 14195 Berlin, Germany

Abstract. We study the distribution of shapes of nodal lines that appear in solutions of the Helmholtz wave equation. For this purpose, we define the density associated with a given shape of a nodal line, and consider its expectation value for Gaussian random fields. We compute the densities of some particular lines, and show that the densities obtained agree well with the predictions of a theory which assumes that the nodal structure of random wave fields can be described in terms of a short-range percolation model. However, we identify closely related quantities, which allow for a clear distinction between the random wave case and a short range ensemble.

PACS numbers: 05.45, 05.40, 03.65

1. Introduction

The nodal domains of a (real) wave function are regions of equal sign, and are bounded by the nodal lines where the wave function vanishes. Even a superficial look at the nodal domains of a quantum wave function reveals the separable or chaotic nature of the quantum system [1]. In separable systems, one observes a grid of intersecting nodal lines, and consequently a checkerboard-like nodal domain pattern. In (quantum) chaotic systems on the other hand, the nodal domains form a highly disordered structure, resembling the geometry found in critical percolation. Blum *et al* [2] argued that also the statistics of the number of nodal domains reflects the fundamental difference between separable and chaotic quantum systems. Bogomolny and Schmit [3] conjectured that the nodal domain statistics of chaotic wave functions in two dimensions can be deduced from the theory of critical percolation. They built a percolation model for the nodal domains which allowed them to calculate exactly the distribution of numbers of domains. Its predictions have been confirmed numerically as far as nodal counting and the area distribution of nodal domains is concerned. While quantum wave functions display long-range correlations, the critical percolation model assumes that such correlations can be neglected on distances of the order of a wave length. One may thus expect that *some* nodal properties in real wave functions are not well described by critical percolation. The main motivation of the present study was to investigate the limits of applicability of the short-range percolation model.

‡ Present address: Institut für Theoretische Physik, Heinrich-Heine Universität Düsseldorf, Universitätsstrasse 1, 40225 Düsseldorf, Germany

The object we will address is related to the distribution of shapes of nodal lines in the random wave ensemble. To be precise, we will calculate the probability, that a nodal line matches a given reference line up to a given precision ϵ.

We will examine the statistics of nodal lines within the random wave model, which is a good description of the eigenfunctions of a quantum billiard in the semiclassical limit [4]. The random wave ensemble consists of solutions of the Helmholtz wave equation for a fixed energy $E = k^2$

$$-\nabla^2\Phi = k^2\Phi. \tag{1}$$

Furthermore the random function Φ is picked up from a Gaussian distribution, i.e. higher order correlations of Φ can be expressed through the two-point correlation function $G_1(r) = \langle\Phi(\boldsymbol{r})\Phi(\boldsymbol{r'})\rangle$ by virtue of Wick's theorem. A convenient representation of Φ is given by the superposition of cylindrical waves with Gaussian distributed amplitudes

$$\Phi(r,\theta) = \sum_m A_m J_m(kr)\exp(im\theta) \tag{2}$$

where $J_m(x)$ are the Bessel functions of the first kind, and r, θ is the position in polar coordinates. The Gaussian random variables obey $A_m^* = (-1)^m A_m$ to render Φ real, and have correlations $\langle A_m^* A_{\bar{m}}\rangle = \delta_{m,\bar{m}}$, $m, \bar{m} \geq 0$. Using the addition theorem for the Bessel functions, one finds for the two-point correlation function

$$G_1(r) = \langle\Phi(\boldsymbol{r})\Phi(\boldsymbol{r'})\rangle = J_0(k|\boldsymbol{r}-\boldsymbol{r'}|) \sim \frac{\cos(k|\boldsymbol{r'}-\boldsymbol{r}| - \pi/4)}{\sqrt{k|\boldsymbol{r'}-\boldsymbol{r}|}}. \tag{3}$$

It displays in fact long-range correlations, which decay with a power law. In order to access the relevance of the long-range correlations, we compare the random wave ensemble with another Gaussian ensemble of random functions, which, however, does not have long-range correlations, and is characterized by the correlation function

$$G_0(r) = \exp(-k^2r^2/4). \tag{4}$$

For the latter ensemble the applicability of the critical (short range) percolation picture is evident [5, 6], since the sign of the random function is not significantly correlated for distances $r \gg k^{-1}$. Figure 1 shows the spatial correlation functions G_0, G_1.

We introduce now briefly the central object of this article. A detailed derivation will be given in section 2. Consider a smooth, closed reference curve $\boldsymbol{r}(s)$ in the plane, which is parameterised by its arclength s. The integral of the square of the amplitude of a random function $\Phi(\boldsymbol{r})$ along this curve

$$X = \frac{1}{2}\int \mathrm{d}s\, \Phi(\boldsymbol{r}(s))^2 \tag{5}$$

is itself a random variable. It samples the function not only at a discrete set of points, but along a one-dimensional subset of the plane. It should be well suited to detect the long range correlations of the random field Φ

Now assume, that Φ has a nodal line very close to the given reference line. Then X will be small in a sense which will be explained later. Thus, by calculating the distribution of X, its cumulants or moments, one obtains the relative importance of the given reference line $\boldsymbol{r}(s)$. We will perform these computations for a circular reference line both for the random wave ensemble and for the short-range ensemble defined above. We will in particular study the scaling properties of the shape probability and of the closely related cumulants of X as a function of the radius (typical size)

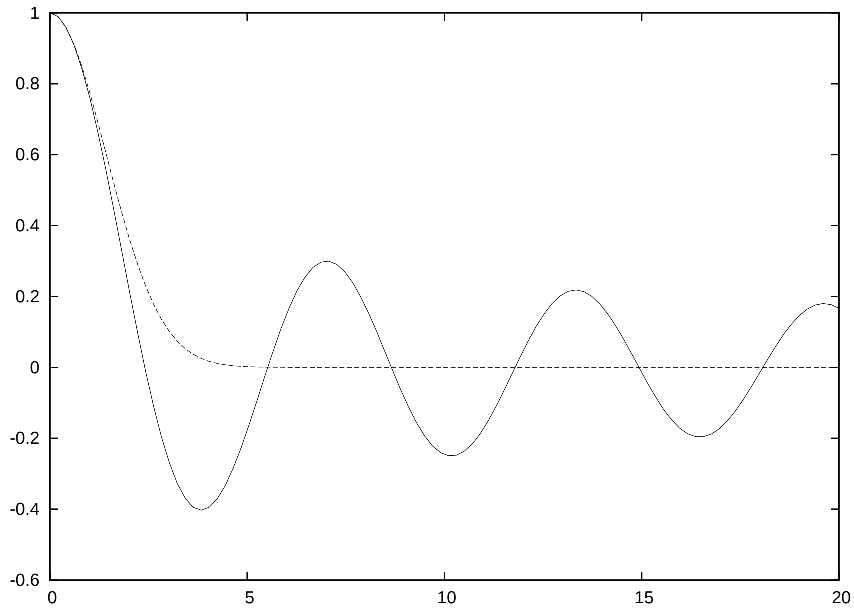

Figure 1. The spatial correlation functions G_1 (solid), and G_0 (dotted) as a function of kr.

of the reference curve. We will see that, although the shape probability does not display relevant differences between random waves and the short-range ensemble, its coefficients, if expanded in terms of the inverse accuracy ϵ^{-1}, show different scaling laws.

The rest of the paper is organized in the following way. The next section describes in detail the new concept which we introduce to the morphological study of nodal lines, that is, the density of line shapes. Once this is done, a formal expression for the density, expressed in terms of X is provided, and computed explicitly for particular shapes - circles (section 3). These densities are evaluated for random waves, and for the short-range ensemble.

2. The density of nodal line shapes

We consider two-dimensional, Gaussian random fields, and a prescribed (closed) reference line. We compute the density of nodal lines which match the reference line in a random wave field. In other words, we compute the probability, that a nodal line with a prescribed form shows up in the Gaussian random wave ensemble. Compared to problems, where the density of (critical, nodal) points of a Gaussian field is calculated [7, 8, 9, 10], we enter here a new dimension and consider the density of one-dimensional strings instead of zero-dimensional, point-like objects. In order to obtain a well-defined and finite theory, we have to regularize the theory by dilating the reference curve to a thin tube with constant thickness d and compute the probability, that a nodal line is completely inside this tube—see Figure (2). Assume now, that a function $\Phi(\boldsymbol{r})$ has a nodal line close to a reference curve $\boldsymbol{r}(s)$, where s denotes the

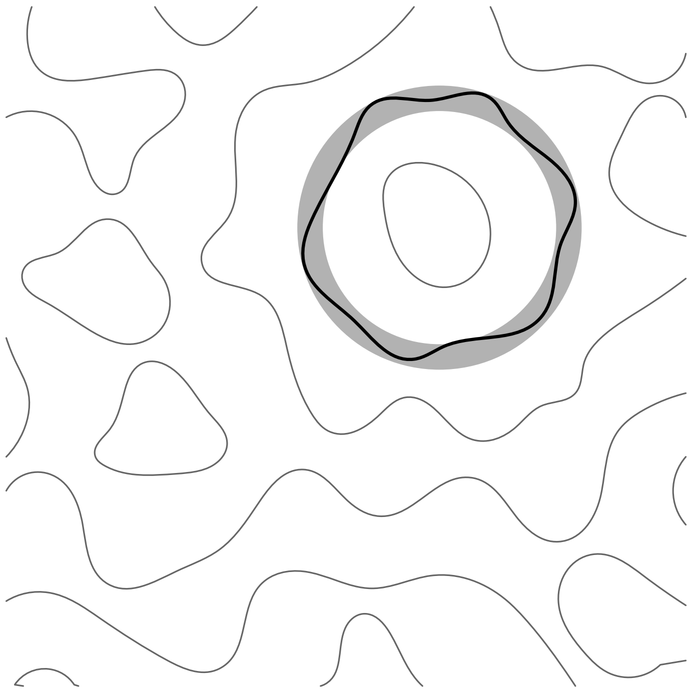

Figure 2. A section of the nodal set of a random wave function. One of its nodal lines lies within the prescribed thin circular tube, i.e. this configuration contributes to the density ρ.

arclength. The normal distance $\eta(s)$ of the nodal line from the reference curve can be obtained via linearization

$$\Phi(\boldsymbol{r} + \eta\boldsymbol{n}) \approx \eta\partial_n\Phi(\boldsymbol{r}) + \Phi(\boldsymbol{r}) = 0 \tag{6}$$

yielding

$$\eta = -\frac{\Phi(\boldsymbol{r})}{\partial_n\Phi(\boldsymbol{r})}. \tag{7}$$

The vector $\boldsymbol{n}(s)$ is normal to the curve $\boldsymbol{r}(s)$. ∂_n denotes the corresponding normal derivative. The probability, that a nodal line lies in a *sharp* tube $|\eta(s)| < d$ is, although well defined, not accessible by analytical means. Therefore, we replace the box shaped cross section by a smooth Gaussian and consider instead the expectation value

$$P_\epsilon = \left\langle \exp\left(-\frac{1}{2\epsilon}\int \mathrm{d}s\, \eta^2\right)\right\rangle \tag{8}$$

where $\int \mathrm{d}s$ is the line integral along the reference line, and $\epsilon = d^3$. However, even the computation of this quantity poses unsurmountable difficulties. $\eta = \phi/\partial_n\phi$ is a ratio of two (in general non independent) Gaussian variables, which is itself non-Gaussian. In order to obtain a tractable expression we approximate the integral $w = \int \mathrm{d}s\, \eta^2$ by a mean-field type expression

$$w_m = \int \mathrm{d}s\, \frac{\Phi^2}{\langle(\partial_n\Phi)^2\rangle} = \int \mathrm{d}s\, \frac{\Phi^2}{\langle(\nabla\Phi)^2\rangle/2} \tag{9}$$

where the latter step requires isotropy of the distribution of the random field Φ. The final expression for the shape probability now reads

$$P_\epsilon = \left\langle \exp\left(-\frac{1}{\epsilon}\int \mathrm{d}s \frac{\Phi^2}{\langle(\nabla\Phi)^2\rangle}\right)\right\rangle = \det\left(1 + \frac{\hat{B}}{\epsilon\,\langle(\nabla\Phi)^2)\rangle/2}\right)^{-1/2} \tag{10}$$

or

$$F(\epsilon) \equiv \log P_\epsilon = -\frac{1}{2}\sum_\mu \log\left(1 + \frac{\beta_\mu}{\epsilon\,\langle(\nabla\Phi)^2)\rangle/2}\right) \tag{11}$$

where $\hat{B}$ is an integral operator with (symmetric) kernel

$$B(s,s') = \langle\Phi(\boldsymbol{r}(s))\Phi(\boldsymbol{r}(s'))\rangle = G(|\boldsymbol{r}(s) - \boldsymbol{r}(s')|) \tag{12}$$

and β_μ are the corresponding eigenvalues. $\hat{B}$ is positive semi-definite and has a *finite* trace $\int \mathrm{d}sB(s,s) = L$, thus its eigenvalues $\beta_\mu \geq 0$ have an accumulation point at zero. The final expression for the logarithm of probability (11) is the starting point of our investigation. It should reflect the relevant features of the inaccessible hard-tube probability, and is an interesting object in its own right§. It takes into consideration the random field Φ along the whole reference curve $\boldsymbol{r}(s)$.

$F(\epsilon)$ is the generating function for the cumulants of the random variable $X = (1/2)\int \mathrm{d}s\,\Phi^2$

$$F(\epsilon) = \log\left\langle\exp\left(-\tilde{\epsilon}^{\,-1}X\right)\right\rangle = \sum_{\nu=1,2,3\ldots}\frac{1}{\nu!}(-1)^{\nu+1}\tilde{\epsilon}^{\,-\nu}\left\langle X^\nu\right\rangle_c \tag{13}$$

where the expansion parameter is $\tilde{\epsilon} = \epsilon\left\langle(\nabla\Phi)^2\right\rangle/2$. It is also the generating function of the traces of powers of the operator $\hat{B}$. In fact, expanding $F(\epsilon)$ in terms of $\tilde{\epsilon}$, i.e. for large $\tilde{\epsilon}$, one finds

$$F(\epsilon) = -\frac{1}{2}\sum_m \log\left(1 + \tilde{\epsilon}^{\,-1}\beta_m\right) = \sum_{\nu=1,2,3\ldots}\frac{1}{2\nu}(-1)^\nu\tilde{\epsilon}^{\,-\nu}\sum_m(\beta_m)^\nu \tag{14}$$

As mentioned in the introduction our goal is to compare two different Gaussian random fields in two dimensions with correlation functions $\langle\Phi(\boldsymbol{r})\Phi(0)\rangle = G(r) = \int \mathrm{d}^2p\,\tilde{G}(p)\exp(i\boldsymbol{p}\cdot\boldsymbol{r})$, namely

$$\begin{aligned} G_1(r) &= J_0(kr) \\ G_0(r) &= \exp(-k^2r^2/4). \end{aligned} \tag{15}$$

G_1 is the correlation function of the usual random wave ensemble with a sharply defined energy k^2. Consequently, it displays long range correlations. G_0 is a typical short-range ensemble. Note that the $\tilde{G}$ are normalized such that

$$\begin{aligned} G(0) = \left\langle\Phi^2\right\rangle &= \int \mathrm{d}^2p\,\tilde{G}(p) = 1 \\ -\nabla^2G(0) = \left\langle(\nabla\Phi)^2\right\rangle &= \int \mathrm{d}^2p\,p^2\tilde{G}(p) = k^2. \end{aligned} \tag{16}$$

This implies an equal nodal line density $\langle|\nabla\Phi|\delta(\Phi)\rangle$ for the long, and short-range ensemble.

§ Private communication with J Hannay.

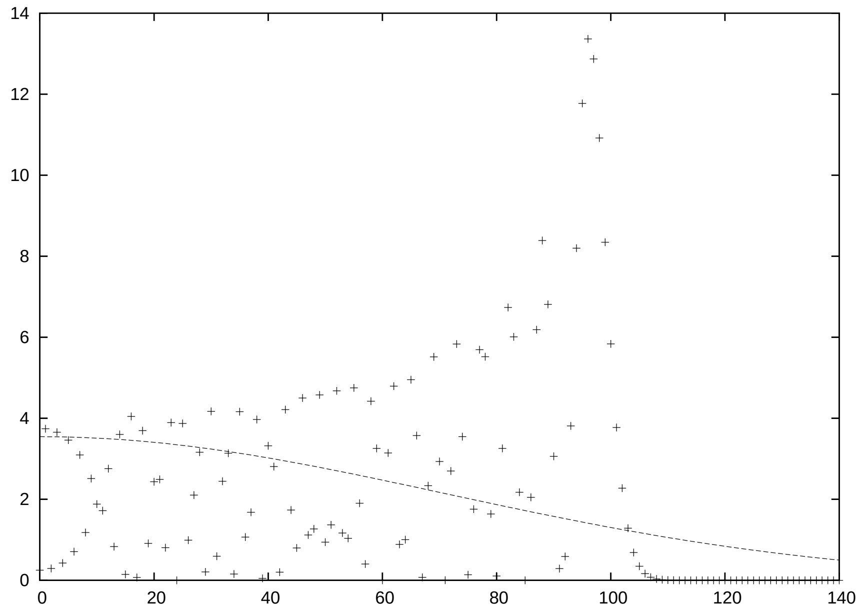

Figure 3. The spectrum of $\hat{B}$ as a function of the order m for $kR = 100$. Shown is the random wave case (symbol $+$), and the short-range case (points are connected to a dotted line).

3. The density of circular nodal lines

We consider now the probability (10) for circles with radius R. The kernel of the operator $\hat{B}$ reads for the random wave ensemble with correlation function G_1

$$B(\theta - \theta') = J_0\left(2kR\sin\left(\frac{\theta - \theta'}{2}\right)\right) \tag{17}$$

where θ, θ' are angles describing positions on the circle. Owing to the rotational invariance of the problem, the eigenfunctions of $\hat{B}$ are $\exp(im\theta), m = 0, \pm1, \pm2, \ldots$. The eigenvalues of the integral operator are therefore

$$\begin{aligned}\beta_m &= R\int_0^{2\pi} \mathrm{d}\theta\, J_0\left(2kR\sin\left(\theta/2\right)\right)\exp\left(im\theta\right) \\ &= 2\pi R\left(J_m\left(kR\right)\right)^2\end{aligned} \tag{18}$$

The eigenvalues for the short range ensemble read

$$\beta_m = 2\pi R\exp(-k^2R^2/2)\, I_m(k^2R^2/2) \approx \frac{2\sqrt{\pi}}{k}\exp\left(-\frac{m^2}{(kR)^2}\right). \tag{19}$$

Figure 3 shows the eigenvalues of $\hat{B}$ for a circle with radius $kR = 100$. The spectrum for the random waves has strong fluctuations, whereas the spectrum for the short-range ensemble is a smooth (almost) Gaussian. It was mentioned before, that the trace obeys $\sum_m \beta_m = L$ for both the short and the long range ensemble.

4. The random wave case

We calculate now $F(\epsilon) = \log P_\epsilon$ and its large ϵ expansion for large radii $R \gg 1/k$. In the region $m < kR$ for large kR the Bessel functions are well approximated by (see [11])

$$J_m(m \sec\beta) \approx \left(\frac{2}{\pi m \tan\beta}\right)^{1/2} \cos\left(m \tan\beta - m\beta - \pi/4\right). \tag{20}$$

By setting $m \sec\beta = kR$, we obtain

$$\begin{aligned} J_m(kR) \approx\ & (2/\pi)^{1/2} \left((kR)^2 - m^2\right)^{-1/4} \\ & \times \cos\left(\sqrt{(kR)^2 - m^2} - m \arccos(m/(kR)) - \pi/4\right). \end{aligned} \tag{21}$$

In the transition region $m \approx kR$, we approximate the Bessel function $J_m(kR)$ in terms of an Airy function $\mathrm{Ai}(x)$ (see [11])

$$J_m(kR) \approx \left(\frac{2}{kR}\right)^{1/3} \mathrm{Ai}\left(\left(\frac{2}{kR}\right)^{1/3} (m - kR)\right). \tag{22}$$

We can combine both asymptotic expansions into a scaling law with a universal scaling function $f(x)$

$$|J_m(kR)| \sim (kR)^{-1/3} f\left(\frac{m^2 - (kR)^2}{(kR)^{4/3}}\right) \tag{23}$$

Figure 4 shows, that the scaling functions $f(x)$ collapse well for three different values of $kR = 50, 100, 200$. Note that for negative arguments the scaling function $f(x)$ is strongly fluctuating. Therefore, $f(x)$ should be understood as a *stochastic* function. $f(x)$ vanishes exponentially for $x \to +\infty$, $f(0) = (2/9)^{1/3}/\Gamma(2/3) = 0.44731$, and $f(x) \sim (-x)^{-1/4}$ for $x \to -\infty$. The eigenvalues of the operator scale according to

$$\beta_m = \frac{2\pi}{k} (kR)^{1/3} \left(f\left(\frac{m^2 - (kR)^2}{(kR)^{4/3}}\right)\right)^2. \tag{24}$$

The leading behaviour of the trace of powers of the operator $\hat{B}$ as a function of the radius R reads

$$\mathrm{Tr}(\hat{B}^\nu) = \sum_m (\beta_m)^\nu \sim k^{-\nu} (kR)^{1+\nu/3} \int_0^\infty \mathrm{d}t \left(f\left((t^2 - 1)(kR)^{2/3}\right)\right)^{2\nu}. \tag{25}$$

We find to leading order in kR

$$\sum_m (\beta_m)^\nu \sim k^{-\nu} \times \begin{cases} kR & \nu < 2 \\ kR \log(kR) & \nu = 2 \\ (kR)^{(1+\nu)/3} & \nu > 2 \end{cases} \tag{26}$$

This scaling behaviour is compared with the corresponding quantity for the short-range correlations, where

$$\sum_m (\beta_m)^\nu \sim k^{-\nu}\, kR \tag{27}$$

for all $\nu > 0$. Some remarks are in order. The moments $\sum_m (\beta_m)^\nu$ show a typical critical behaviour for the random wave case. Below the critical power $\nu^* = 2$, the large kR-scaling does not differ from the short-range case. At the critical power, logarithmic deviations show up, and above ν^*, the trace $\sum_m (\beta_m)^\nu$ displays an anomalous scaling

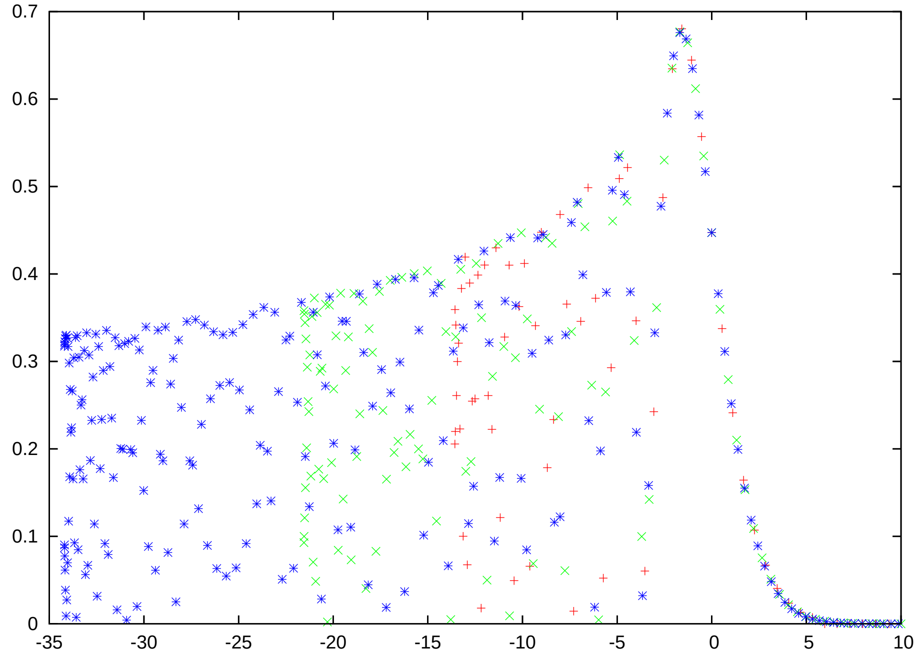

Figure 4. The scaling function $f(x)$ for $kR = 50$ (red $+$), $kR = 100$ (green $\times$), and for $kR = 200$ (blue $*$).

in kR, different from the non-critical, short-range ensemble. Now we return to the shape probability

$$\log P_\epsilon \approx -(kR)\int_0^\infty \mathrm{d}t \log\left(1 + \omega^{-1}(kR)^{1/3}\left(f\left((t^2-1)(kR)^{2/3}\right)\right)^2\right) \tag{28}$$

where $\omega = \epsilon k^3/(4\pi)$ is the dimensionless width of the tube around the (here circular) reference curve. The limit of *small* ω corresponds to the moment (25) for $\nu \searrow 0$ as far as the scaling behaviour is concerned. Therefore, $\log P_\epsilon$ cannot be considered as a "good" quantity to distinguish between the long range and the short-range case — for both ensembles, $\log P_\epsilon \sim kR$. There might be anomalous higher order corrections in the random wave case which are not considered here. On the other hand, a large-ϵ expansion (which means arbitrarily wide tubes) yields the sequence of cumulants (25) for integer ν which in fact have characteristic scaling properties for $\nu \geq 2$. Figure 5 shows a log–log plot of the third cumulant ($\nu = 3$) as a function of the radius kR for $10 < kR < 200$. The slope is 1.34063 (standard error = 0.065%), i.e. confirms the predicted exponent 4/3.

5. Conclusion

In this paper we compared Gaussian random waves Φ and a short-range ensemble of random fields by investigating the statistics of $(1/2)\int \mathrm{d}s\, \Phi^2$ along a given reference curve. The ν−th order cumulants of this random variable obey non-trivial scaling laws with respect to the linear size of the reference curve (here circles of radius R) in

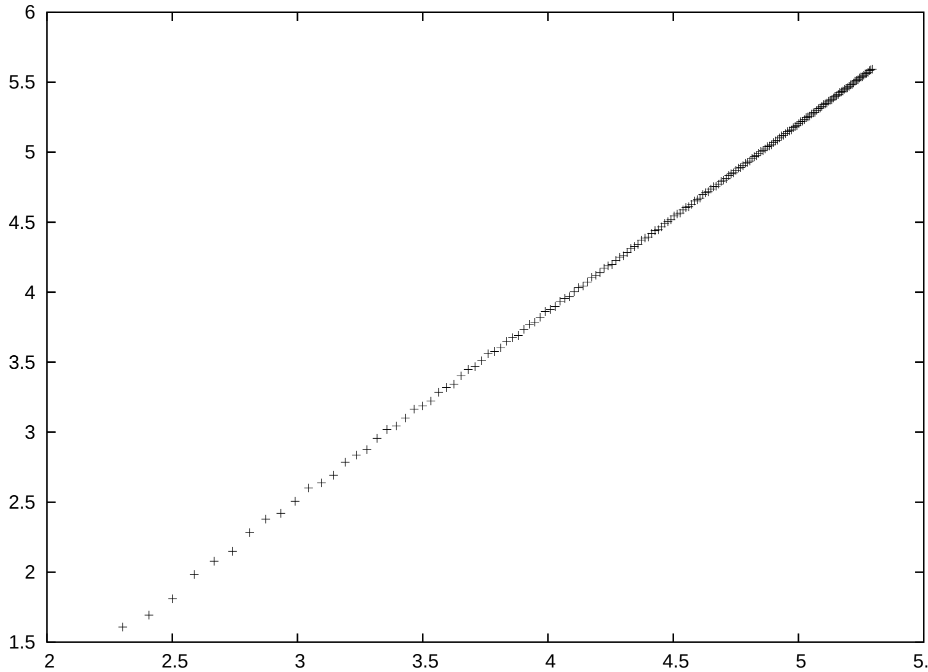

Figure 5. Log–log plot of the third cumulant $\sum_m (\beta_m)^3$ as a function of the radius $10 < kR < 200$ for the random wave case.

case of the long-range random waves. The second order cumulant shows logarithmic deviations from the corresponding scaling behaviour of the short-range ensemble. The cumulants of order three and higher have non-trivial exponents. Namely, these cumulants scale like $R^{(1+\nu)/3}$, whereas the cumulants for the short-range ensemble scale $\sim R$. The probability, that a nodal line lies in a circular tube of given thickness ϵ, however, turned out to be a less useful candidate to probe the long range properties of the random functions. The logarithm of the shape probability for the short and the long range case scale in exactly the same manner, which might explain the success of the ad-hoc model [3].

Acknowledgments

We would like to thank N Sondergaard, M Dennis, J Hannay and B Gutkin for many useful discussions. This work was supported by the Einstein Center and the Minerva Center for non-linear Physics at the Weizmann Institute, the Israel Science Foundation, and the EU TMR project "Mathematical Aspects of Quantum Chaos".

References

[1] Richard M. Stratt, Nicholas C. Handy, and William H. Miller. *On the quantum mechanical implications of classical ergodicity. J. Chem. Phys.* **71,** 3311–3322, 1979.

[2] Galya Blum, Sven Gnutzmann, and Uzy Smilansky. *Nodal Domains Statistics: A Criterion for Quantum Chaos. Phys. Rev. Lett.* **88,** 114101, 2002.

[3] E. Bogomolny and C. Schmit. *Percolation Model for Nodal Domains of Chaotic Wave Functions. Phys. Rev. Lett.* **88,** 114102, 2002.

[4] M. V. Berry. *Regular and irregular semiclassical wavefunctions. J. Phys. A: Math. Gen.* **10,** 2083–2091, 1977.

[5] Richard Zallen and Harvey Scher. *Percolation on a Continuum and the Localization-Delocalization Transition in Amorphous Semiconductors. Phys. Rev. B* **41,** 4471–4479, 1971.

[6] Abel Weinrib. *Percolation threshold of a two-dimensional continuum system. Phys. Rev. B* **26,** 1352–1361, 1982.

[7] M. V. Berry and M. R. Dennis. *Phase singularities in isotropic random waves. Proc. R. Soc. Lond. A* **456,** 2059–2079, 2000.

[8] M. R. Dennis. *Phase critical point densities in planar isotropic random waves. J. Phys. A: Math. Gen.* **34,** L297303, 2001.

[9] Georg Foltin. *The distribution of extremal points of Gaussian scalar fields. J. Phys. A: Math. Gen.* **36,** 4561–4580, 2003. math-ph/0301041.

[10] M. R. Dennis. *Correlations and screening of topological charges in gaussian random fields. J. Phys. A: Math. Gen.* **36,** 6611–6628, 2003. arXiv: math-ph/0302024.

[11] M Abramowitz and I. A. Stegun, editors. *Handbook of Mathematical Functions.* United States Department of Commerce, 1964. 10th printing 1972.